

VARIABLE STARS IN THE CLUSTER NGC 6882/6885

by

Amanda O. Henderson

A senior thesis submitted to the faculty of

Brigham Young University

in partial fulfillment of the requirements for the degree of

Bachelor of Science

Department of Physics and Astronomy

Brigham Young University

April 2008

Copyright © 2008 Amanda O. Henderson

All Rights Reserved

BRIGHAM YOUNG UNIVERSITY

DEPARTMENT APPROVAL

of a senior thesis submitted by

Amanda O. Henderson

This thesis has been reviewed by the research advisor, research coordinator, and department chair and has been found to be satisfactory.

\_\_\_\_\_  
Date

\_\_\_\_\_  
Eric Hintz, Advisor

\_\_\_\_\_  
Date

\_\_\_\_\_  
Eric Hintz, Research Coordinator

\_\_\_\_\_  
Date

\_\_\_\_\_  
Ross Spencer, Department Chair

## ABSTRACT

### VARIABLE STARS IN THE CLUSTER NGC 6882/6885

Amanda O. Henderson

Department of Physics and Astronomy

Senior Thesis

This thesis presents time-series photometric data on the open star cluster NGC 6882/6885 based on archival observations from 2004. Out of 228 stars selected four variable stars were observed, two previously known, and two previously suspected. Light curves created from reduced frames suggest that SU Vulpeculae is a possible binary system with orbital period of 45 days and its primary star is a pulsator with period of 0.1751 days and amplitude of 0.0019. Previous analysis by Hintz & Rose (2005) suggests that V382 Vulpeculae is a  $\beta$  Cephei star. This analysis gives a period of 0.4249 days and amplitude of 0.0046 for V382 Vulpeculae. Star 2 in this ensemble is identified as Star 13 in Hintz & Rose (2005) as a possible  $\delta$  Scuti with a period of 0.0776 days and amplitude of 0.015. This analysis gives a period of 0.0723 days and amplitude of 0.0152. Star 1 in this ensemble is a previously suspected high amplitude pulsator with a period of 0.2029 days and amplitude of 0.2108. This analysis confirms the period for Star 1.

## ACKNOWLEDGMENTS

I would like to thank my research advisor Dr. Eric Hintz for his invaluable guidance. This paper would not have happened without his help and patience. I would also like to thank Paul Iverson and Craig Swenson for their IRAF scripts. Without them I'd be here another six months. I truly am grateful for my parents. They have been a constant support.

# Contents

<b>Acknowledgments</b>	<b>v</b>
<b>Table of Contents</b>	<b>vi</b>
<b>List of Tables</b>	<b>viii</b>
<b>List of Figures</b>	<b>ix</b>
<b>1 Introduction</b>	<b>1</b>
1.1 History of the Cluster . . . . .	1
1.2 Why Variables? . . . . .	2
1.3 Motivation . . . . .	3
<b>2 Background</b>	<b>4</b>
2.1 Variable Stars . . . . .	4
2.1.1 Intrinsic . . . . .	4
2.1.2 Extrinsic or Line-of-sight Variables . . . . .	5
2.1.3 Naming Scheme . . . . .	5
2.2 Filters . . . . .	6
2.3 Imaging Devices . . . . .	8
<b>3 Observations and Reductions</b>	<b>10</b>
3.1 Observations . . . . .	10
3.1.1 Telescope . . . . .	10
3.1.2 Plate Scale and Field of View . . . . .	11
3.2 Calibration Frames . . . . .	14
3.2.1 Bias . . . . .	14
3.2.2 Darks . . . . .	15
3.2.3 Flats . . . . .	17

3.3	IRAF . . . . .	17
3.3.1	Reduction Process . . . . .	18
3.4	VARSTAR . . . . .	20
3.5	Period04 . . . . .	21
<b>4</b>	<b>Analysis and Conclusions</b>	<b>22</b>
4.1	Analysis . . . . .	22
4.1.1	SU Vulpeculae . . . . .	22
4.1.2	V382 Vulpeculae . . . . .	22
4.1.3	Star 2 - Previous Star 13 . . . . .	24
4.1.4	Star 1 . . . . .	25
4.2	Conclusion . . . . .	26
	<b>References</b>	<b>27</b>

## List of Tables



## List of Figures

1.1	HR Diagram . . . . .	2
2.1	Electromagnetic Spectrum . . . . .	7
2.2	Plank curves . . . . .	7
3.1	Map of Region 2 - Southwest Corner . . . . .	12
3.2	Map of Region 3 - Southeast Corner . . . . .	13
3.3	Map of Region 4 - Northeast Corner . . . . .	14
3.4	Averaged Zero Frame . . . . .	15
3.5	Averaged Dark Frame . . . . .	16
3.6	Averaged Flat Frame . . . . .	18
4.1	Phase Diagram for SU Vul with Published Period . . . . .	23
4.2	Phase Diagram for SU Vul with Current Period . . . . .	23
4.3	Phase Diagram of V382 Vul with Published Period . . . . .	24
4.4	Phase Diagram of V382 Vul with Current Period . . . . .	24
4.5	Phase Diagram of Star 2 with Published Period . . . . .	25
4.6	Phase Diagram of Star 2 with Current Period . . . . .	26
4.7	Phase Diagram of Star 1 with Current Period . . . . .	26

# Chapter 1

## Introduction

### 1.1 History of the Cluster

The clusters NGC 6882 and NGC 6885 are found in the constellation Vulpecula at a Right Ascension (RA) of 20:11:48.00 and a Declination (Dec) of +26:49:00. Since 1930 there has been much debate on how to appropriately define these clusters. It is widely recognized that there are two groups of stars in the area. The debate lies in how to define those two groups. Trumpler (1930) originally described the clusters NGC 6882 and NGC 6885 as a single cluster, stating that NGC 6882 was a condensation inside of NGC 6885. Thirty years later, Johnson et al. (1961) described them as NGC 6882 being the cluster and NGC 6885 as not being a cluster at all. That same year Svolopoulos (1961) reported that NGC 6885 was an association around 6882. Johnson et al. (1961), Svolopoulos (1961), and Becker & Fenkart (1971) all reported a general distance to the clusters of approximately 600 parsecs (pc). However, recently Robichon et al. (1999) reported a distance of  $397 \pm 50$  pc. And Platais et al. (2003) reported a distance of over 1 kpc. Parsecs are the unit of measurement most commonly used by astronomers. A parsec is equal to  $3.086 \times 10^{16}$  meters or 3.26 lightyears.

In Hintz & Rose (2005) they report on a variable star search in the northeast quadrant of the cluster. They examined the 3 known variables in that region and reported 5 new variables and 8 suspected variables. They also discuss the extent of the cluster and the idea that the cluster is actually two, or perhaps three, clusters of different distances superimposed. In Polleck et al. (2004) a search for variables is reported in the region to the north of the Hintz & Rose (2005) region. Given the previous success in finding variable stars in this cluster it is important to search the other three quadrants to look for additional variables.

## 1.2 Why Variables?

A Hertzsprung-Russell (HR) diagram is a diagram that plots a stars spectral type vs its magnitude (level of brightness). This type of diagram shows stellar evolution in a nutshell. There is a connection between a type of variation in a stars brightness and its stage of stellar evolution (see Figure 1.1). Some stars pass through several stages of variability in its evolutionary path, and others remain completely stable until their death, at which point they become a one time variable. Given the timing of the observations in this study we will be most likely to find the  $\delta$  Scuti or  $\gamma$  Dor stars that are shown in Figure 1.1.

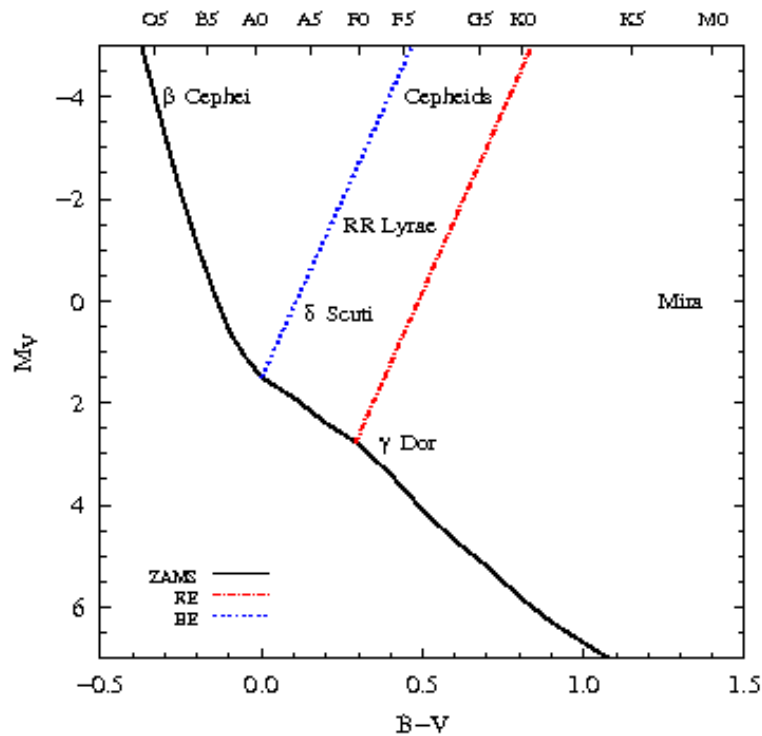


**Figure 1.1:** General placement of Variable star types with respect to main sequence stellar evolution.

In addition to finding pulsating variables as discussed above it is also possible to find eclipsing binary systems. Again with the time scales of our data set these would most likely be W Ursae Majoris systems. A challenging aspect of eclipsing binary systems is that they can be found throughout the HR diagram.

### **1.3 Motivation**

The identification and classification of variable stars in the region will lead to a proper classification for the clusters NGC 6882 and 6885. Studying the number and type of variables along with their location in the cluster will help in understanding the evolution of the stars in the cluster and the evolution of the cluster itself. Most stars go through a phase of variability during their evolution. By studying the variable stars in this region we can further our understanding of stellar evolution.

Since  $\delta$  Scuti variables are distance indicators a large enough sample could be used to definitively separate the various clusters in terms of distance. Their spatial distribution could be used to define the ‘edges’ of each cluster. Since the first region studied by Hintz & Rose (2005) provided a number of new  $\delta$  Scuti variables there is hope to find more in the remaining three regions.

## Chapter 2

### Background

#### 2.1 Variable Stars

Variable stars are stars whose measured radiation varies over time in some way. There are two main categories of Variable stars, Intrinsic Variables and Extrinsic variables. Within these main groups there are many subdivisions. The subdivisions are often named after the first stars identified to vary in such a manner. Below we will examine each class of variable stars we might expect to see in these clusters.

##### 2.1.1 Intrinsic

A star is placed in the intrinsic category if the cause of variability is due to changes in the physical properties of the star itself. This category is divided into two to three main groups depending on the source of the variation.

The first group is pulsating stars. This group consists of stars whose atmospheres undergo periodic expansion and contraction. Stars that vary in a manner similar to  $\delta$  Cephei are called Cepheids. Stars that vary in a manner similar to RR Lyrae are classified as RR Lyrae stars. These two classes fall into the classical instability strip as was shown earlier in Figure 1.1. Outside of the classical instability strip are other classes of pulsating stars such as  $\beta$  Cephei, Mira, and semi-regular variables, some of which are also shown in Figure 1.1.

The second group is eruptive or explosive variables. This group consists of stars that exhibit sudden and dramatic changes such as flares or mass ejections. These objects are called cataclysmic variables, since the cause of the brightness change can literally disrupt the entire star. Many times novae and supernovae are placed in this category, although they can also be considered a category of their own.

### 2.1.2 Extrinsic or Line-of-sight Variables

A star is placed in the extrinsic category if the cause of variability is due to external properties such as rotation or eclipse. These are systems where the light of sight can have a major impact on what we see. Unlike intrinsic variables where observers from different places would see effectively the same thing, only if you are in the right place would you see the changes in the extrinsic variables.

Eclipsers are usually binary star systems, but can sometimes contain planetary systems which cause the light variation. Binary systems are classed as variable stars because as one companion eclipses the other there is a decrease in the total luminosity of the system and this occurs on a periodic basis. There are a wide variety of eclipsing variable systems based on the period of the orbit and the distance between the two stars.

The second group in this category is stars whose light varies due to rotational phenomenon. Some examples are large sunspots, or an extremely fast rotation which caused the star to become ellipsoidal. This shape results in a non-uniformed radiation output.

### 2.1.3 Naming Scheme

The German astronomer Johan Bayer devised a naming scheme for the stars. He began with the brightest star in a constellation and assigned it the Greek letter  $\alpha$  followed by the genitive form of the Latin name for the constellation.

Friedrich W. Argelander began naming variable stars following the pattern set by Bayer. The first variable star found in a constellation is designated by the letter R, as this is the first letter not used by the Bayer naming scheme. Variable stars in the constellation are given the letters R through Z in order of discovery, followed by the genitive form of the Latin name for the constellation.

Once Z is reached the double letters are used RR to RZ, SS to SZ, all the way to ZZ. Once ZZ is reached the double letters AA to AZ, BB to BZ up to QZ is

used. The letter J is not used because of possible confusion with the letter I. This letter combination scheme allows for 334 variables. When there are more than 334 variables in a constellation the naming then switches to V (for variable), the number 335, 336 etc. in order of discovery, followed by the genitive form of the Latin name for the constellation.

At first novae were not included in this naming scheme. They were simply designated by the constellation name and the year that it occurred. Today novae are included in the variable naming scheme. Some earlier novae have been renamed to fit within this scheme.

## 2.2 Filters

All radiation is part of the electromagnetic spectrum. This spectrum is what astronomers refer to as light. It is organized by wavelength. The longest wavelengths being radio waves and the shortest being gamma rays (see Figure 2.1). Visible light, the light that we see with our eyes, is in the range of about 800 to 400 nanometers.

Most stars radiate over the complete range of the electromagnetic spectrum. The manner in which a star radiates is described by a Plank curve. Max Plank determined a curve that describes the radiation of body called a blackbody. This is a theoretical object that absorbs all radiation incident upon it while radiating energy back out. Although stars are not blackbodies they radiate in a manner nearly identical to blackbodies. It is this relation that allows us to use a Plank curve to describe stellar radiation over the entire electromagnetic spectrum.

Because stars radiate over the entire spectrum it is common to use filters. Filters are a piece of glass or plastic that is designed to allow only certain wavelengths of light to pass through. The use of filters isolates a wavelength and allows for the intensity of that specific wavelength to be measured. For example, a V filter allows visual light that is radiated from a star to pass through to a detector.

A star will radiate differently in different wavelengths. Therefore different measurements will be taken when different filters are used. This difference between

filter measurements is used to create a color index. This color index can then be used to determine information about the star's temperature. This is because there is a correlation between color and temperature. The filters used in this research were Johnson VRI filters. These are broadband filters that pass more light. This makes exposure times shorter, but also gives less detailed information.

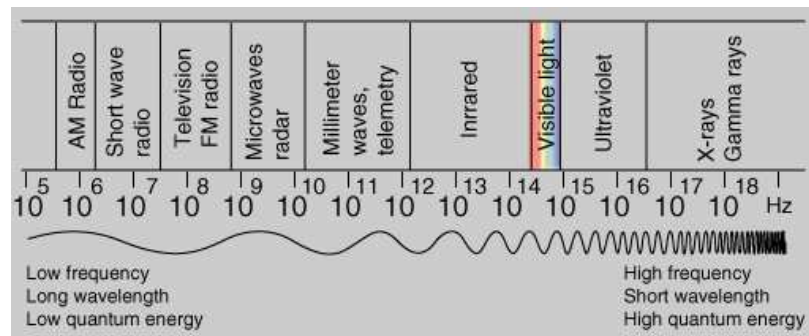


**Figure 2.1:** Electromagnetic Spectrum

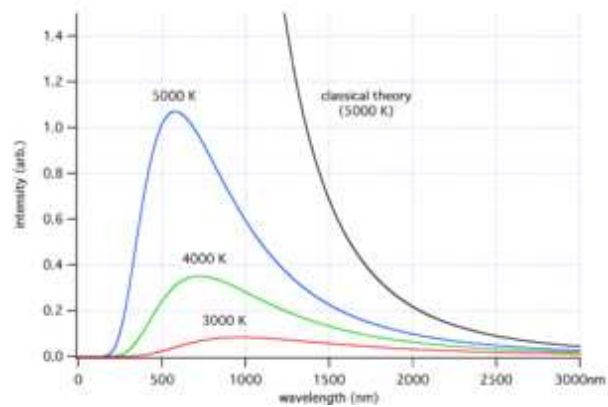


**Figure 2.2:** The relationship between wavelength (color) and temperature



### 2.3 Imaging Devices

Imaging devices are what are used to measure a stars radiation by counting photons. The first imaging device used in astronomy was the eye. The measurement of a stars radiation at a certain wavelength is called the stars magnitude. Hipparchus was the first to devise the magnitude scale. Using his eyes he assigned the brightest stars a magnitude of 1 and the faintest a magnitude of 6. As well as there being a limit to the number of stars that can be seen with the naked eye, there is no permanent image produced.

The first permanent images were produced by photographic plates. Although photographic plates were a vast improvement over the eye, there were also many disadvantages. Most photographic plates were large glass sheets that had to be handled with care. Also only about one percent of the photons incident on the plates were counted due to the inefficiency of film. Another disadvantage is that film does not respond to light in a linear manner.

Another way to count photons is to use Photomultiplier Tubes. Photomultiplier tubes amplify the signal received when a photon hits the detector with reasonable efficiency. This amplification decreases the exposure time necessary. Statistically Photomultiplier tubes are the best per observation. However, they too have some disadvantages. With a Photomultiplier tube only one object at a time can be imaged, and only with good sky conditions. Good sky conditions include no clouds, uniform temperature around the telescope, and uniform light in the sky. Nights that meet all three of these conditions are called photometric nights. Photometric nights can be hard to come by.

Currently, the most commonly used imaging device is the Charged Coupling Device camera (CCD). The general public uses CCD cameras in their digital cameras and video cameras. Researchers use a higher quality CCD chip. A CCD chip is a grid of photon counters that act as wells. When the CCD camera takes a frame the photon counters turn the light into electrons that collect in these “wells”.

Through a standard data reduction process these electron counts are turned into magnitudes. CCDs collect over 75% of the photons that strike them. In some wavelengths they can record up to 95% of the photons that strike the chip. However, using a CCD also requires many calibration frames, as even unexposed to light there are electrons in the wells of the chip. For this research the Ap47 CCD was used to collect data.

## Chapter 3

### Observations and Reductions

#### 3.1 Observations

##### 3.1.1 Telescope

A telescope is made of a series of lenses or mirrors that gather light and focus it on to an imaging device. The two basic types of telescopes are refracting telescopes which use lenses to focus light, and reflecting telescopes which use mirrors to focus light.

Refracting telescopes have two lenses, an objective lens and an eyepiece lens. The objective lens brings an image into focus at its focal point. The eyepiece lens brings the image from the focal point to the observer. There are a few disadvantages to refracting telescopes. The total length of the telescope is the focal length of the objective lens added to the focal length of the eyepiece lens. The larger the objective lens is the longer the telescope must be. There is also a limit to the size of refracting telescopes. The lenses are made of glass. A glass lens can be no larger than about 1.5 meters before they will collapse under their own weight. Lenses also cause chromatic aberration. This is color distortion due to different wavelengths focusing at different points.

Reflecting telescopes use a series of mirrors to collect and focus light onto a detector. There are four types of reflecting telescopes: Prime focus, Newtonian, Cassegrain, and Coude.

A prime focus reflector has no secondary mirror; a detector must be inserted into the tube of the telescope at the focal point to the mirror. A Newtonian reflector has a flat secondary mirror. This secondary mirror is set at an angle to redirect the light out of the tube to a detector.

A Cassegrain reflector has a convex secondary mirror at the focal point of the primary. The convex mirror redirects the light back toward a hole in the primary mirror. This effectively folds the focal length of the primary mirror so that the tube does not need to be so long.

A Coude reflector has a convex secondary mirror that acts like the secondary in a Cassegrain. A Coude also has a flat tertiary mirror that redirects the light out the side of the tube.

The focal ratio of a telescope is the ratio of the focal length to the aperture. The effective focal length of a telescope is determined by multiplying the diameter of the primary mirror by the denominator of the focal ratio.

The Orson Pratt Observatory (OPO) is home to the David Derrick Telescope (DDT) is a 16 inch (406 mm) primary mirror telescope. The OPO is located on the 5th and 6th floors of the Eyring Science Center at Brigham Young University. This telescope is used by faculty and students as the primary tool for research and observational astronomy classes at BYU. The DDT has a Newtonian and Cassegrain focus. At the Newtonian focus the DDT has a focal ratio of  $f/4$  and an effective focal length of 1624 mm. At the Cassegrain focus the DDT has a focal ratio of  $f/12.5$  and an effective focal length of 5075 mm. For this research the DDT was used at the Cassegrain focus.

### **3.1.2 Plate Scale and Field of View**

The Plate Scale is the ratio between two objects to the linear distance between their images on a photographic plate. Roughly, it is an indicator of how large an object will appear in your detector. Plate scale is usually reported in arcseconds per millimeter. One radian is equal to 206,265 arcseconds. Plate scale is equal to 206,265 arcseconds divided by the effective focal length.

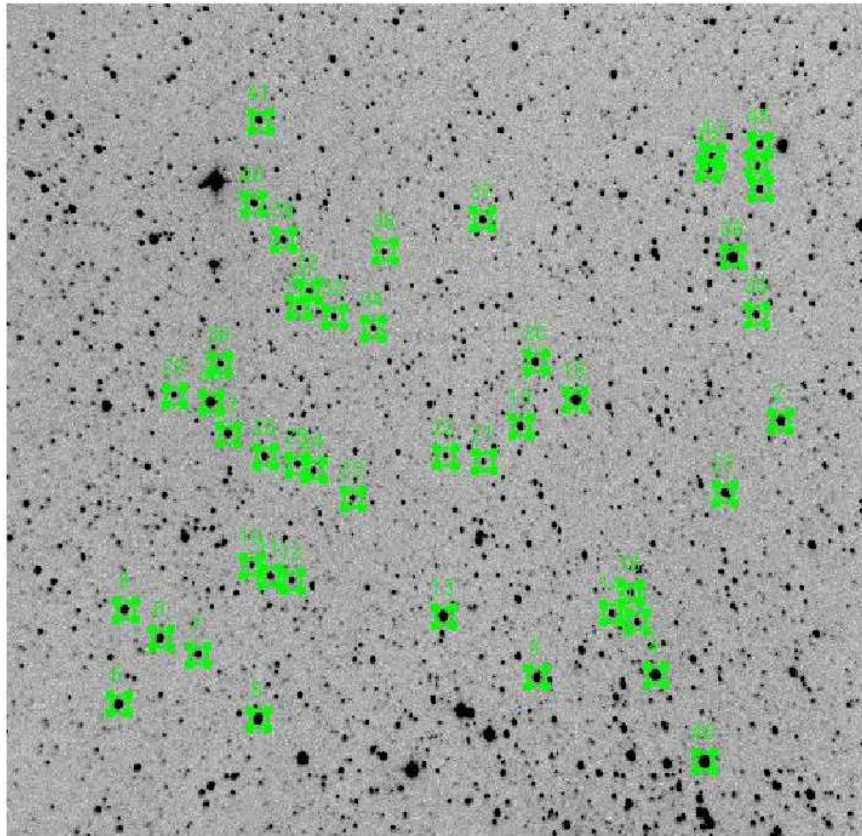


**Figure 3.1:** Region 2 (Southwest Region) of NGC 6882/6885.

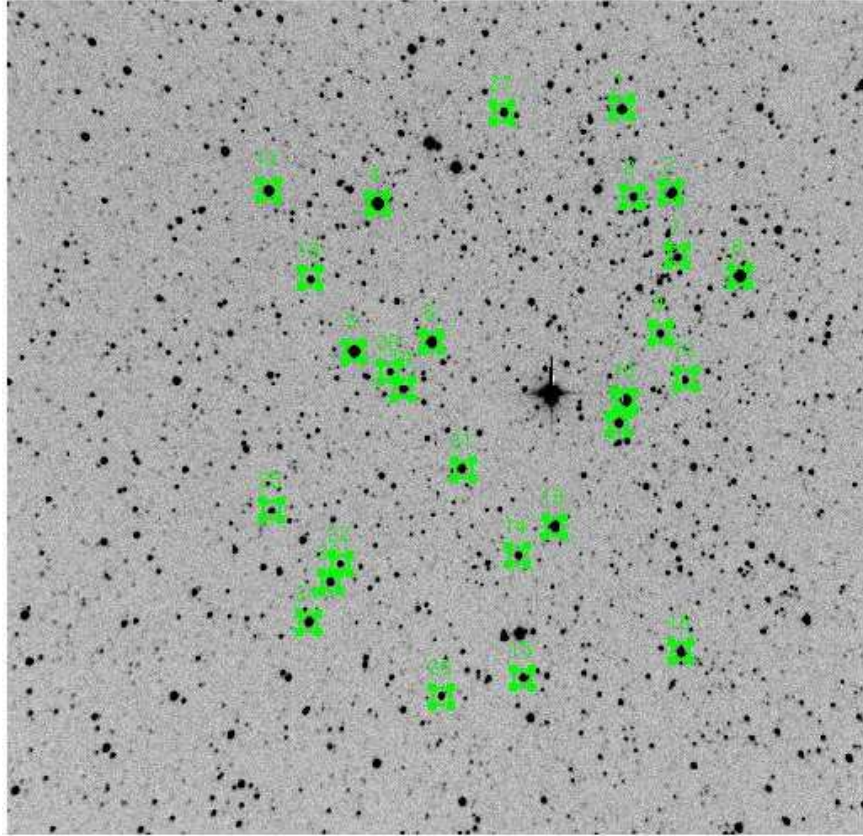


**Figure 3.2:** Region 3 (Southeast Region) of NGC 6882/6885.

The DDT at the Newtonian focus has a plate scale of 127.01 arcseconds per millimeter, and 40.64 arcseconds per millimeter at the Cassegrain focus. The plate scale multiplied by the pixel size of the CCD chip gives the amount of sky that can be imaged by that particular chip/telescope combination. The DDT at the Newtonian focus with the Ap47p images about 1.64 arcseconds per pixel. Since NGC 6882/6885 is covers a large section of sky it was subdivided into 4 regions. With Region 1 being the northwest corner (Hintz & Rose 2005), Region 2 the southwest corner (see Figure 3.1), Region 3 the southeast corner (see Figure 3.2), and Region 4 the northeast corner (see Figure 3.3). Region 2 was the primary focus of the research.

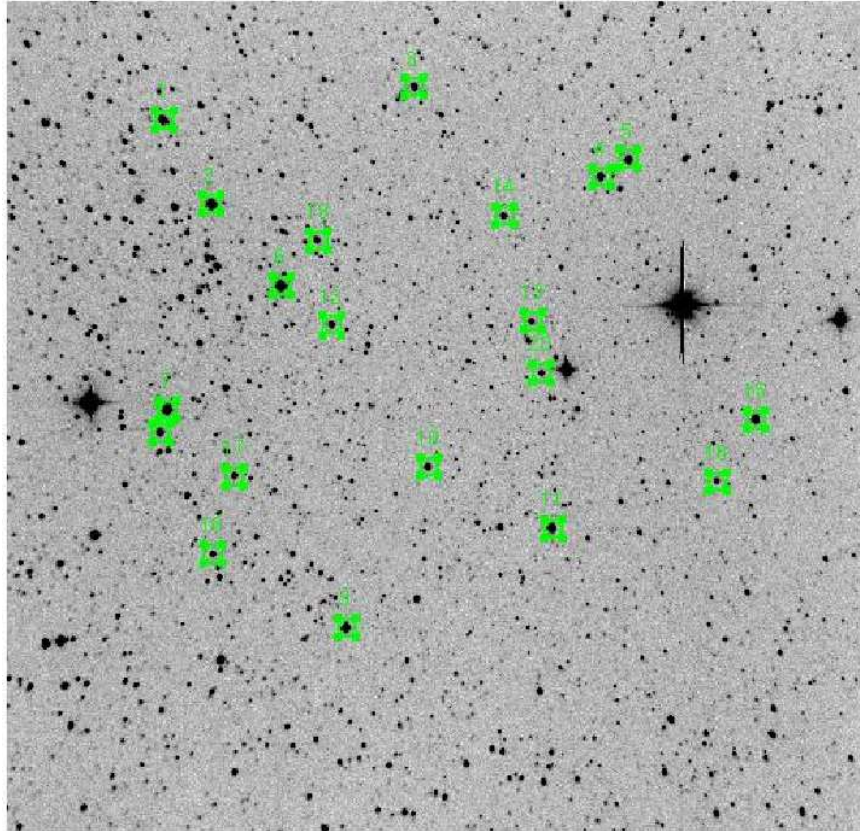


**Figure 3.3:** Region 4 (Northeast Region) of NGC 6882/6885.

## 3.2 Calibration Frames

Because CCD chips convert photons into electricity they must be calibrated in order to get a true measurement and not just a machine's response to itself. The sections Bias, Darks, and Flats explain each step of calibrating the CCD chip.

### 3.2.1 Bias

Even if the CCD has not been exposed to light there will still be electrons in the “wells”. This is simply because the CCD is electronically powered and there is a constant base level flow of electrons through the chip. Bias frames are often referred to as Zero frames. These frames are named such because they are an exposure of

zero length of time. These frames establish the base level of electrons in each “well”. These frames are averaged and then the average Zero frame is then subtracted from all Dark frames.

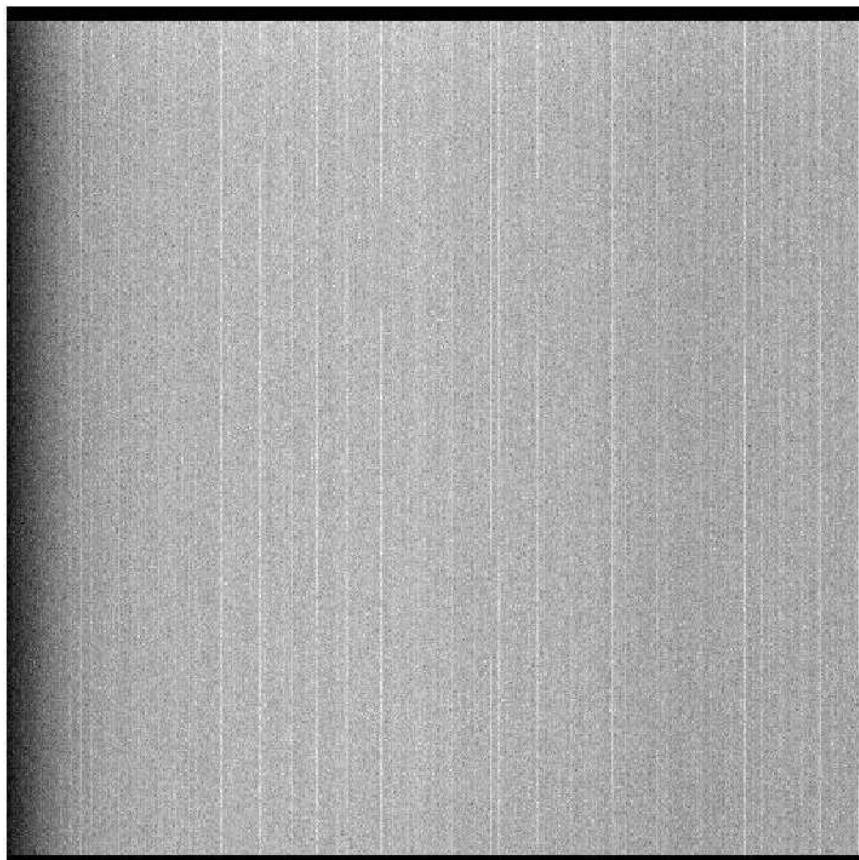


**Figure 3.4:** Averaged Zero frame

### **3.2.2 Darks**

In order for the CCD chip to work there must be a current applied. Because of this current it is possible for electrons that were not converted from photons to enter the wells. In order to correct for this possibility, exposures are taken with the



shutter closed. This establishes the CCD chip's response to the current applied, this is called the Dark Level. Because the shutter is closed all electrons in the wells either come from the base level established by the Zero frames, or from the current.

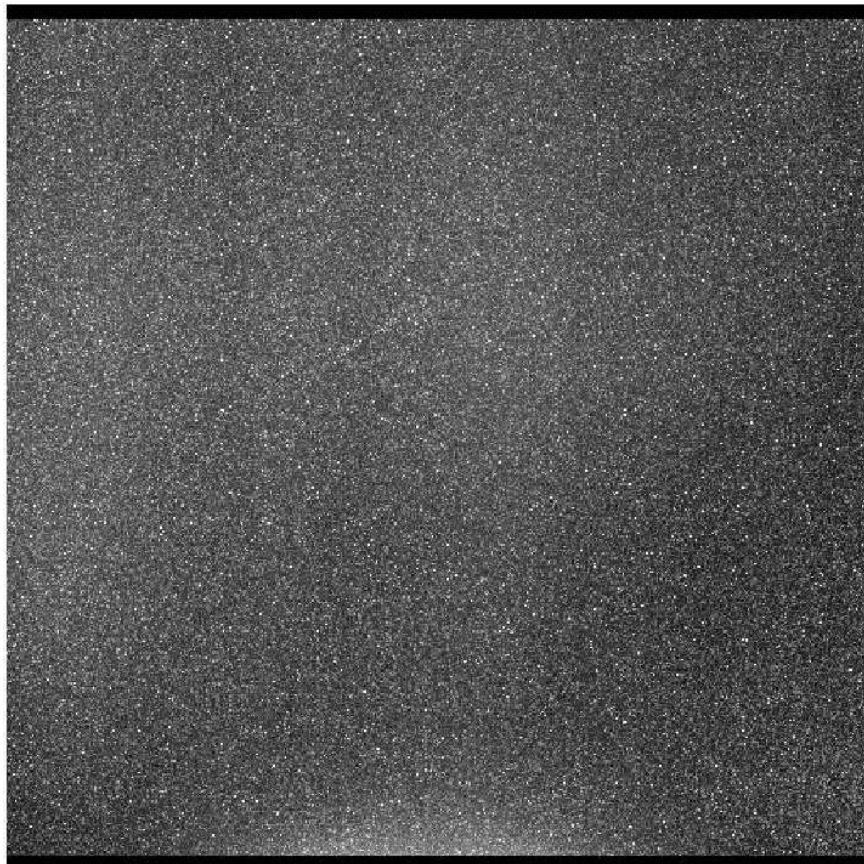


**Figure 3.5:** Averaged Dark frame with averaged Zero frame subtracted

Dark levels can be affected by the operating temperature of the CCD. High quality research grade CCD generally have liquid nitrogen cooled systems and can run at temperatures of  $-70^{\circ}$  to  $-110^{\circ}$  C ( $-94^{\circ}$  to  $-166^{\circ}$  F). At these temperatures there is almost no dark current. The CCD used for this research was the Ap47 run

at an average temperature of  $-22^{\circ}$  C. Even at this temperature there is a significant dark current of a couple of electrons per second.

Because the objective of these frames is to see how the CCD responds to the current applied over time, exposure times for Dark frames is roughly equal to the desired Object frame exposure time. The averaged Zero frame is subtracted from each dark frame and then the Dark frames are averaged.

### **3.2.3 Flats**

Every pixel, or well, is different and responds differently to light. To correct for this response difference a Flat field is used. Flat fields are difficult as a field of uniform brightness over the entire chip area is needed.

Many different ways to accomplish this have been used by astronomers over the years. The most common types of flat fields are dome flats and twilight flats. When dome flats are used a blank flat screen is uniformly illuminated inside the dome. The telescope is then pointed at the screen and a short exposure is taken in each filter to be used. When twilight flats are used, the astronomer selects a patch of sky that is mostly uniform in brightness. This patch of sky must not be too bright and must be free of stars and other objects. The astronomer then takes a series of exposures of this patch of sky in all filters to be used. Twilight flats were used for this research.

The averaged Dark frame is then subtracted from these Flat frames. The flat frames are then averaged according to filter and then subtracted from each Object frame according to filter.

## **3.3 IRAF**

IRAF stands for Image Reduction and Analysis Facility. It was created under a government contract at the National Optical Astronomy Observatories (NOAO). It is a free image processing program that can be downloaded from the internet. UNIX or LINUX operating systems are required to use it. It is command line code software where the user must type what you want it to do. IRAF is often used in conjunction

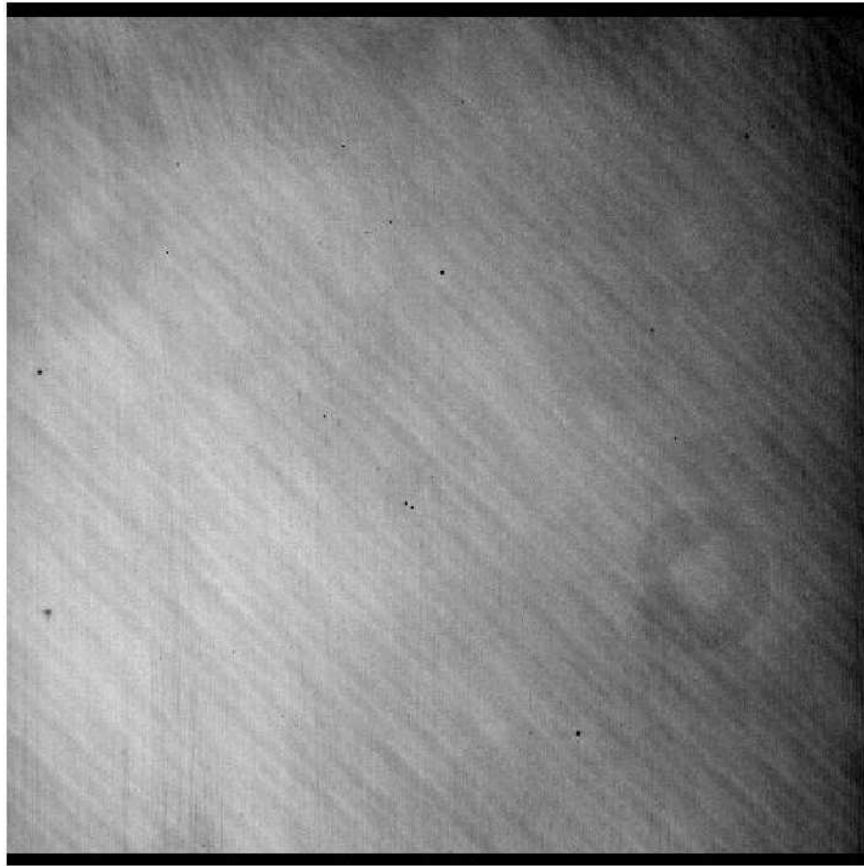


**Figure 3.6:** Averaged Flat frame in the V filter with averaged Zero and averaged Dark frame subtracted

with DS9. DS9 is a display window which allows the user to: view the telescope frames, change the contrast of the image, and mark object positions

### 3.3.1 Reduction Process

A script is a small program that tells IRAF what to do. The data for this research was reduced using scripts written by Paul Iverson and Craig Swenson. The first step was to run scripts that calculated the gain and noise levels in each filter. The software used to run the telescope stores the image and relevant information together in one file called a FITS file. The command *rfits* in IRAF converts these fits files to individual IRAF images. This command creates an image file and a header

file. The image file is the image frame, and the header file contains all information regarding that frame such as: observation time, observation location, and filter.

Though the headers contain pertinent information, they usually do not include all information necessary and must be edited to include all missing information. This was done using three scripts. Among other things these scripts: calculated and inserted the Heliocentric Julian Date (HJD) and the air mass, inserted the RA, DEC, gain and noise levels, and insure the image type designation is correct.

The full width at half maximum (FWHM) refers to the measure of the full width of a curve at half of its maximum height. This theoretically gives about 63% of the curve and cuts off the potentially noise contaminated wings. IRAF's *psfmeasure* command calculates a point spread curve of the stars in the frame and then calculates the FWHM. A script was run to calculate and insert the FWHM into the header of each frame. This, along with the gain and noise levels calculated earlier further reduces the possibility of false readings.

After all important information was included in the headers the Zero, Dark and Flat frames could be averaged and applied as detailed earlier in the paper. An object frame that has had zero, dark and flat frames subtracted from it is called a reduced frame. The edges of the reduced object frames were then trimmed. This is like cutting off the fringe so that the edges are smooth.

Due to the rotation of the earth, stars move throughout the night, just like the sun does during the day. Because of this, a telescope must be able to track, or move with the object it is centered on. Due to imperfect tracking systems an object isn't always found in the same place on each frame. This is called drift. To correct for drift a script was run to align all frames. This script selects fixed points on a frame and finds those points on every other frame. It then shifts all the frames to align the fixed points. Aligning the frames makes photometry much simpler.

Photometry is the process by which the photon counts are translated into magnitudes. There are two types of photometry packages in IRAF: DAOPhot and aperture photometry. *DAOPhot* was developed by Peter Stetson at the Dominion

Astrophysical Observatory (DAO). This package is generally used for crowded fields. The program is designed to separate stars that are close together and give better values. Aperture photometry is the simplest type of photometry. It consists of defining the area to be measure, summing the photon counts inside the surface and then subtracting a sky count to get the total counts. For this research aperture photometry was used.

### 3.4 VARSTAR

VARSTAR is a program written by Dr. Eric Hintz (Hintz 2007). This program calculates differential magnitudes for stars based on extracted data from the output file created by the PHOT command. This extracted data includes the star identification based on the order number from the coordinate file, the magnitude, observation time, airmass and the filter.

In its fifth version, VARSTAR creates a “super star” based off of the average magnitude value of the ensemble. The ensemble consists of the same stars that were marked for *photing*. The program then compares the magnitude of each star in the ensemble to the “super star” and calculates the differential error. Stars with large errors have significant magnitude variations. The stars with large errors are then removed from the ensemble and the “super star” is recalculated and the process is repeated.

This continues until the errors are less than one one hundredth. If stars that are known to be stable stars are used in the comparison ensemble, they should be the ones left in the ensemble when the process is complete.

The program then calculates the differential magnitude for all stars selected in the field and outputs those magnitudes into individual files for each star. These files can them be graphed. These graphs are light curves. They show graphically how the flux of a star is changing with time. Variable stars have distinctive light curves. Pulsates have light curves that appear similar to a sine wave. Eclipsers have a steady line with a shallow dip and then a deeper dip. Through careful review of the graphs

of each star selected for the ensemble potential variable stars can be identified for further analysis.

### 3.5 Period04

The light curves created by graphing the differential magnitude vs. the Heliocentric Julian Date, (HJD) are complex waves. The period of the curve is found by the relation  $1/f$ , where  $f$  is the primary frequency of oscillation. To find the primary frequency of oscillation, the data set is run through Period04. The program Period04 uses a discrete Fourier algorithm to mathematically extract individual frequencies from multiperiodic time sets. Several frequencies can be pulled from a single data set. Once several frequencies are found a phase plot is made to determine which frequency is the primary frequency. The phase is determined by taking the decimal part of the equation . The differential magnitude is then plotted vs. this phase.

Each night of data catches a different part of the curve. A data set is said to be in phase when all components of the curve align to form a sinusoidal curve. This happens at the primary frequency. Once the primary frequency is found the period is found by taking the inverse of the frequency.

## Chapter 4

### Analysis and Conclusions

#### 4.1 Analysis

##### 4.1.1 SU Vulpeculae

In the General Catalogue of Variable Stars (2004) (GCVS), SU Vulpeculae is listed as a long period red variable. The only reported period for this star is 45 days. When a phase plot is created using this period, the plot has the appearance of an eclipser. However, the dips are too shallow to be a companion star. If this is an eclipser, it is possible that the companion star's orbital plain is at an angle to our line of sight. Another less likely possibility is that the companion could be a planet. Whether a binary system or not, the primary star is a pulsator. A Fourier decomposition of this data set produces a period of 0.2438 days with amplitude of 0.0036. More data is necessary to confirm these results. A phased diagram using the published period of 45 days is shown in Figure 4.1, while a phase diagram with the new period is shown in Figure 4.2.

##### 4.1.2 V382 Vulpeculae

V382 Vulpeculae is reported as a spectral type of B3 V and classified as a  $\beta$  Cephei star by Hintz & Rose (2005). It is located in the center of the cluster and found in all four regions. Hintz & Rose (2005) reported a period of 0.1808 days while this research reports a period of 0.4249 days. This is almost 2.4 times longer than the previously reported period. This research also reports amplitude of 0.00455476, which is 2.4 times smaller than the previously reported amplitude of 0.011. Only data in the V filter was analyzed. In order to correctly determine the period of this variable, more data must be taken and an O-C diagram created. Figure 4.3 shows the

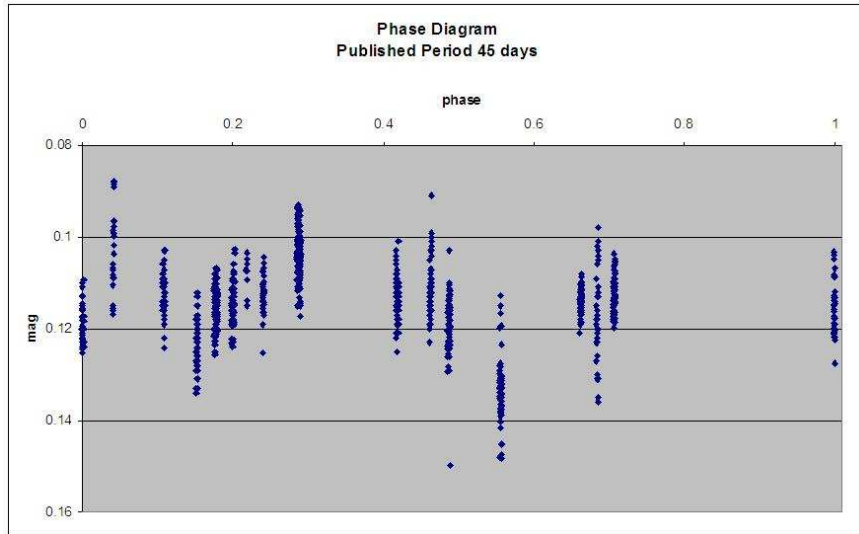


**Figure 4.1:** Phase diagram created using the published period of SU Vulpeculae.

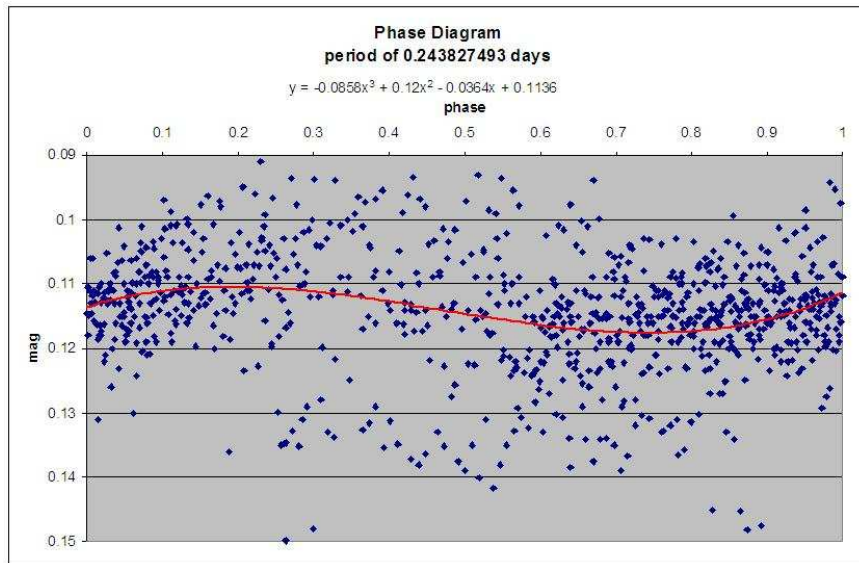


**Figure 4.2:** Phase diagram created using the period given by current data for SU Vulpeculae.

data phased with the period published in Hintz & Rose (2005). The phased diagram generated with the period determined from this data set is shown in Figure 4.4.



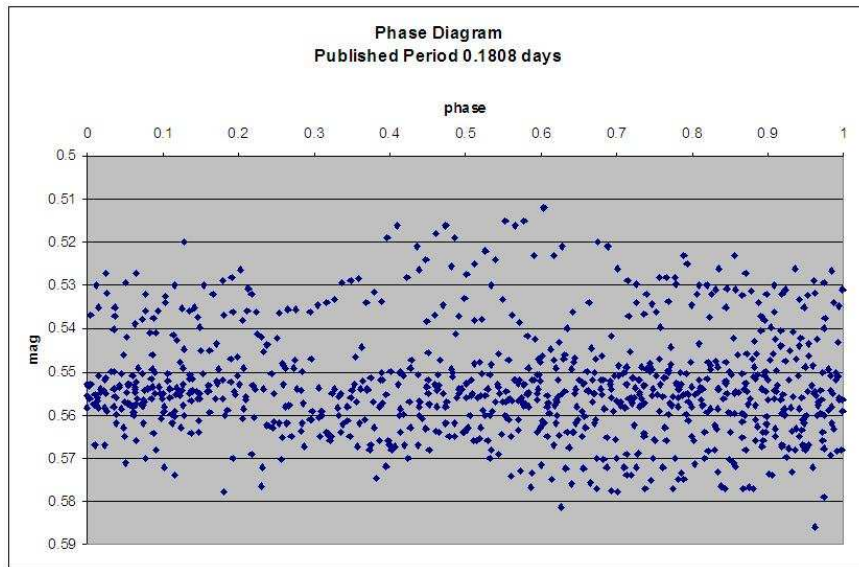


**Figure 4.3:** Phase diagram created using the published period for V382 Vulpeculae.

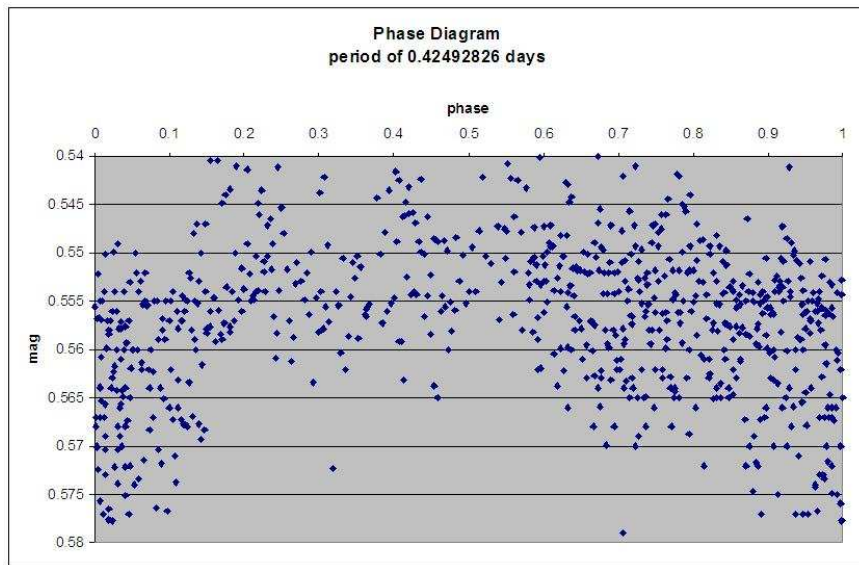


**Figure 4.4:** Phase diagram for V382 Vul created using the period determined from the current data set.

#### 4.1.3 Star 2 - Previous Star 13

Star 2 is reported as Star 13 by Hintz & Rose (2005). This research confirms the 0.0776 day period with a difference of 0.005. This equates to about 7 minutes

difference. This research also confirms the amplitude of 0.015 in the V filter. Hintz & Rose (2005) reports the star as a spectra type F3. More data in many filters is required to confirm this classification. Again the phase diagrams are shown in Figures 4.5 and 4.6.

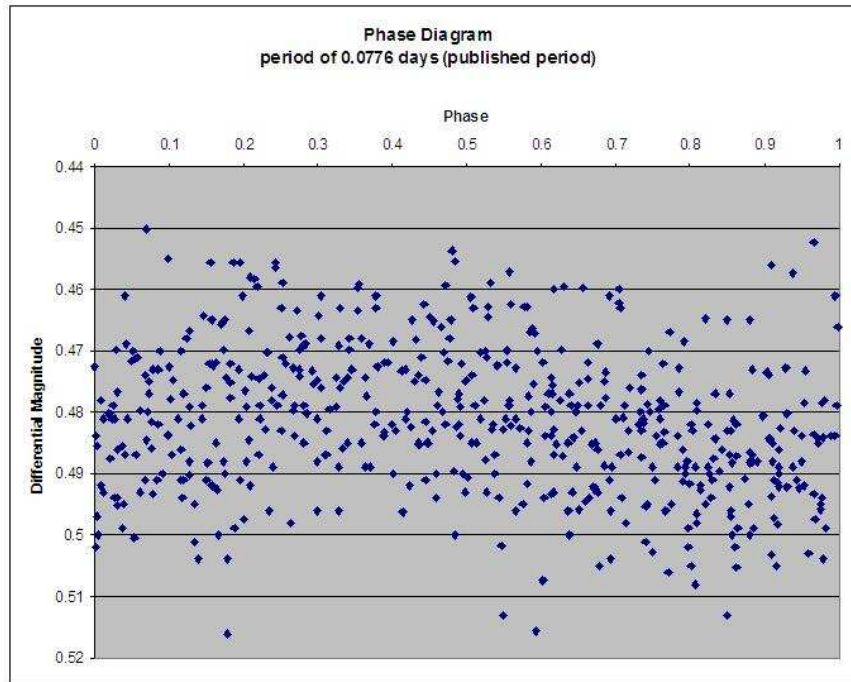


**Figure 4.5:** Phase diagram created using the published period for Star 2.

#### 4.1.4 Star 1

Star 1 is reported as a high amplitude pulsator with a period of 0.2056 days by Polleck et al. (2004). This research confirms a period of 0.2029 days with a difference of 0.0027 from the published period. This equates to about 3.8 minutes. More data is needed to obtain a spectral classification. The phased diagram for the new data is shown in Figure 4.7.

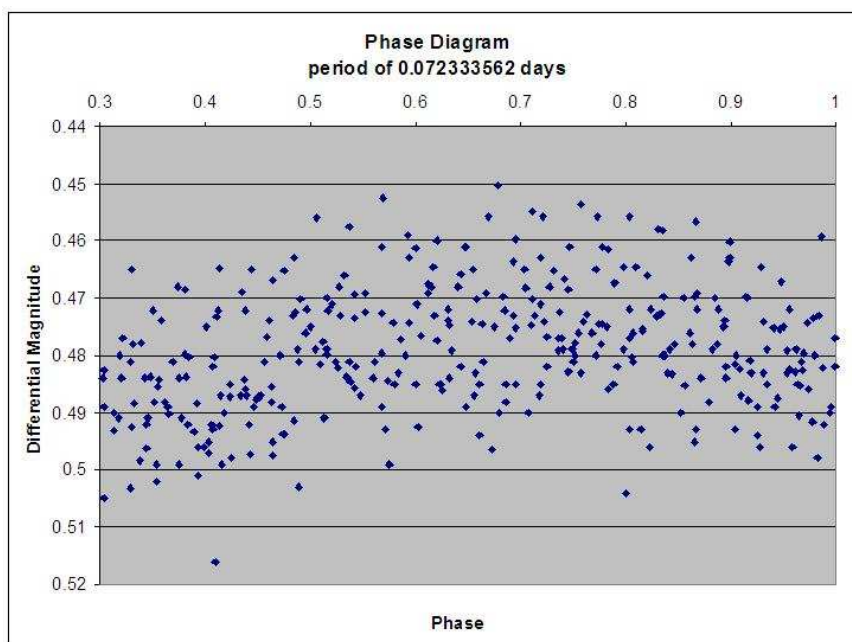


**Figure 4.6:** Phase diagram created using the period determined from the current data set.

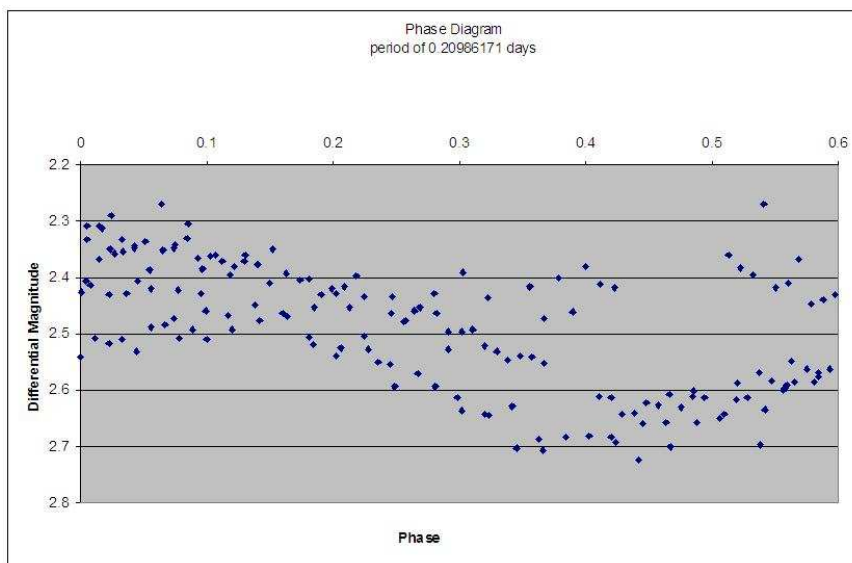


**Figure 4.7:** Phase diagram created using the period given by current data.

## 4.2 Conclusion

There is much to be learned about the cluster NGC 6882/6885 and its variable stars. In addition to the four variable stars<sup>26</sup> found and analyzed in this research, there

are many other variable stars in the cluster NGC 6885. More data and a more rigorous reduction is required to gain enough information to correctly classify the variables and the clusters in this region.

## References

- Becker, W. & Fenkart, R. 1971, *A&AS*, 4, 241
- General Catalogue of Variable Stars 2004,  
(<http://www.sai.msu.su/groups/cluster/gcvs/gcvs/iii/vartype.txt>)
- Hintz, E.G. 2006, private communications
- Hintz, E.G. & Rose, M.B., 2005, *PASP*, 117, 955
- Johnson, H.L., Hoag, A.A., Iriarte, B., Mitchell, R.I., & Hallam, K.L. 1961, *LowOB*, 8, 255
- Platais, I., Kozhurina-Platais, V., Barnes, S.A., Reid, I.N., Belfort, M., Sperauskas, J., Dzervitis, U. & Bronnikova, N.M. 2003, *BAAS*, 203, 1411
- Polleck, J.E., Hintz, E.G., & Ruppeiner, G. 2004, *BAAS*, 205, 2202
- Robichon, N., Arenou, F., Mermilliod, J.-C., & Turon, C. 1999, *A&A*, 345, 471
- SIMBAD database 2006, (<http://simbad.harvard.edu/cgi-bin/WSimbad.pl>)
- Svolopoulos, S.N. 1961, *ApJ*, 134, 612
- Subramaniam, A., Mathew, B. & Kartha, S.S. 2006, *BASI*, 34, 315
- Trumpler, R.J. 1930, *LicOB*, 14, 154